

GENERAL  ELECTRIC
GENERAL ELECTRIC COMPANY
CORPORATE RESEARCH AND DEVELOPMENT
P.O. Box 43, Schenectady, N.Y. 12301 U.S.A.

**PERMANENT MAGNET AC DISC MOTOR
ELECTRIC VEHICLE DRIVE**

G.B. Kliman



400 COMMONWEALTH DRIVE WARRENDALE, PA 15096

SAE Technical Paper Series

830111

Permanent Magnet AC Disc Motor Electric Vehicle Drive

Gerald B. Kliman

General Electric Co.
Corporate Research & Development
Schenectady, NY

International Congress & Exposition
Detroit, Michigan
February 28 - March 4, 1983

The appearance of the code at the bottom of the first page of this paper indicates SAE's consent that copies of the paper may be made for personal or internal use, or for the personal or internal use of specific clients. This consent is given on the condition, however, that the copier pay the stated per article copy fee through the Copyright Clearance Center, Inc., Operations Center, 21 Congress St., Salem, MA 01970 for copying beyond that permitted by Sections 107 or 108 of the U.S. Copyright Law. This consent does not extend to other kinds of copying such as copying for general distribution, for advertising or promotional purposes, for creating new collective works, or for resale.

Papers published prior to 1978 may also be copied at a per paper fee of \$2.50 under the above stated conditions.

SAE routinely stocks printed papers for a period of three years following date of publication. Direct your orders to SAE Order Department.

To obtain quantity reprint rates, permission to reprint a technical paper or permission to use copyrighted SAE publications in other works, contact the SAE Publications Division.

Permanent Magnet AC Disc Motor

Electric Vehicle Drive

Gerald B. Kliman

General Electric Co.
Corporate Research & Development
Schenectady, NY

ABSTRACT

The principal objective of this work was to establish the feasibility of the axial flux permanent magnet ac disc motor with load-commutated inverter as a candidate for an electric passenger vehicle drive system component.

Three motors were built in the course of the project. The first, known as the proof-of-principle (POP) motor, was built to demonstrate the electromagnetic concepts and establish design data. It was built with rare earth magnets and a dc motor type random winding. The second motor, known as the Functional Model A [FM(A)] motor, was built for full performance and high speed (11,000 rpm). Alnico 8E magnets were used to stimulate manganese-aluminum. A three-layer air gap winding was used in the stator. This motor did not perform as predicted due primarily to demagnetization of the magnets and, secondarily, to imbalance in the windings. The third motor, known as Functional Model B [FM(B)], corrected these problems by use of rare earth magnets and a novel, single-layer chain winding. The motor performed well and in excess of contract requirements electromagnetically, thermally, and mechanically. A peak efficiency of 93% was measured at cycling power when the motor was being driven by the inverter. Several modifications were proposed to raise the efficiency to 95%.

THE HISTORY OF ELECTRIC PASSENGER VEHICLES has been, for the most part, an account of the application of dc commutator motors operating from battery banks mediated by some form of controller which was usually a switched resistor set. With the advent of solid-state power electronics and medium scale integrated logic, other forms of control (and thereby other forms of motors, particularly ac motors) became practical.

This project started with an internal GE study (1)* of possible electric vehicle drives. The conclusions of that study were as follows:

1. For the near term, the conventional dc motor with a transistor chopper was the best prospect.
2. In the intermediate term, an induction motor with transistor inverter offered improvements in cost, weight, and efficiency.

* Numbers in parentheses designate references at end of paper.

3. For the far term, with considerably less knowledge and higher risk, an axial flux disc-type permanent magnet motor with load-commutated SCR inverter might offer improvements beyond that of the induction motor drive.

At the time, the dc motor-transistor chopper system was under development for the DOE electric test vehicle ETV-1.(2,3) Subsequent to the internal study, NASA/Lewis Research Center and DOE requested proposals for advanced electric vehicle drives. The work reported here on the permanent magnet ac disc motor for electric vehicle drive was based on the far-term option described above. In parallel, the induction motor drive of the intermediate term option was undertaken in a second contract and is reported separately.(4,5)

The motor proposed for this study may be described, very generally, as an inside-out permanent magnet, disc-type synchronous motor with air gap windings. A sketch of the motor concept is shown in Figure 1. A photograph of a cut-away model is shown in Figure 2 to illustrate the proper relationship of the motor components. The magnetic field is supplied by permanent magnets mounted in the rotor. The rotor is made of a nonmagnetic material. The stators are radial arrays of conductors, with appropriate end turns and connections, fixed in a nonmagnetic, insulating matrix. The wound stator discs are fixed to the frame. To provide a return path for the magnetic fluxes, laminated steel plates are positioned outboard of the stator discs.

EXPLODED VIEW OF DISK MOTOR (ONE SIDE)

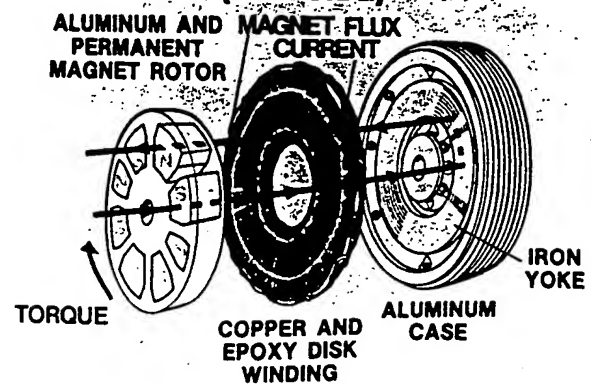


Figure 1. Structure of the AC Disc Machine



Figure 2. Full-Scale Model of Proof-of-Principle Motor

In this motor concept, the objectives for the design of an electric vehicle motor may be achieved. Efficiency will be high over the entire operating cycle since there will be no excitation or slip loss and very little iron core loss. Weight will be low because most of the heavy iron flux paths and the copper field windings have been eliminated. The frame may be a light-weight aluminum die-casting. Production cost may be low since the fabrication of the components should be relatively simple and done "in the open." For example, contrast the wire lay-down and casting required with conventional methods of winding wires into the slots of a small bore stator. With the possible exception of the magnets, materials costs should also be low because high-quality thin steel laminations and coil insulation may not be required. Commutating inductance (as well as noise) should be low because of the absence of slots and because of the large air gap. The motor will also run at leading power factor. These properties allow the use of a relatively inexpensive, lightweight load-commutated inverter (LCI) utilizing commercially available thyristors. The permanent magnet rotor can be built for higher speed operation than earlier dc disc motors with windings on the rotor, thus providing a further opportunity for weight reduction. Finally, since there are no commutators, slip rings, brushes, or exposed end windings, no maintenance (other than for the bearings) is required, and reliability should be very high.

Preliminary studies (1) showed that the permanent magnet disc motor with load-commutated SCR inverter could yield significant gains in system weight, efficiency, and vehicle range, as summarized in Figure 3.

REQUIRED PERFORMANCE

The vehicle weight, geometry, and performance requirements were similar to other experimental vehicles or drive system developments and are summarized in Table 1.

The performance requirements for FM(B) are summarized in the shaft torque-speed curve shown in Figure 4. The upper curve in Figure 4 represents the so-called "diesel equivalent" specification.

POWER SUPPLY

In order to minimize inverter size, there must be mediation between the linearly increasing ac voltage of the motor and the fixed dc voltage of the battery. The means for accomplishing this are shown schematically in the circuit diagram of Figure 5. The chopper regulates the dc link voltage by time ratio control between zero and full battery voltage, which would usually be

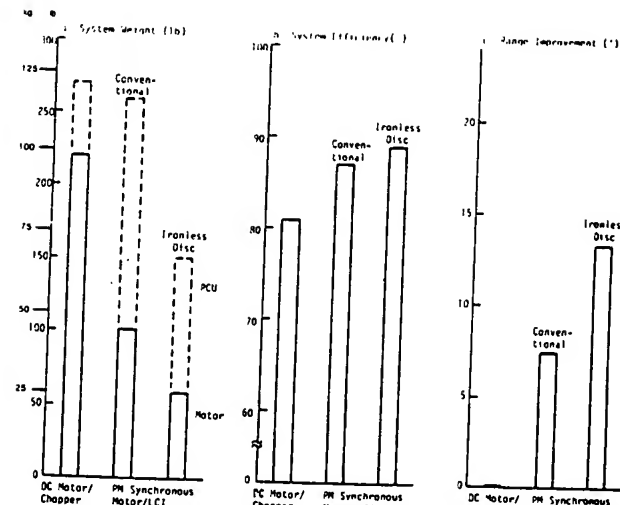


Figure 3. Propulsion System Comparison Summary

reached near the start of the constant power region shown in Figure 4 (in this case, about 5000 rpm). Above this speed, the dc link current is constant. The motor voltage, however, continues to rise with increasing speed. The difference is taken up by phasing back the inverter. This action is summarized in Figure 6.

The inverter circuit of Figure 4 does not require auxiliary thyristors and circuitry for commutation, as a more than a sufficient amount of permanent magnets are used in the motor so that overexcited operation is the normal mode. This means that the motor operates at leading power factor, which in turn means that the voltage at the motor terminals becomes negative before the line current goes through zero. If the gate trigger signal is removed from the thyristor before this point, it will turn off and stay off until the voltage becomes positive again. A more detailed explanation of this principle may be found in References 6 and 7. The elimination of commutation circuits allows the construction of a very efficient, low-cost, compact, and lightweight inverter.(6,7) An auxiliary commutation system is required to deliver torque at zero speed and start the motor. This may be achieved by interrupting the dc link with the chopper or by means of an auxiliary commutation circuit, as shown in Figure 5. These auxiliary means are required up to about 10 percent of base speed (i.e., full dc link voltage) at which point the motor is generating sufficient voltage to commutate the inverter.

The control system for the inverter/motor system is similar to that for the flywheel system described in References 6 and 7.* An outstanding feature of this system is that no shaft position sensor is required. All of the required control information is derived from the motor terminal voltage and line currents.

It is characteristic of the load-commutated inverter that the inductance of the motor limits performance by its role in the commutation process. In general, higher speeds and higher efficiency will be achieved as the motor inductance is reduced. The PM/ac disc motor concept results in an extremely low inductance which makes it a good match for the load-commutated inverter.

PROOF-OF-PRINCIPLE MOTOR

Several different forms of disc motor are possible. A concept selection study was made which resulted in the recommenda-

* The inverter and control system modified for use in these tests were developed under Lawrence Livermore Laboratory subcontract No. 8990503, Mr. Thomas Barlow, Contract Monitor

Table 1
Performance Requirements

<i>Contractual</i>	
Cruise 2 hours at 88.5 km/h (55 mph)	
SAE J227a schedule D repeated for 2 h	
10% uphill grade at 56.3 km/h (35 mph) for 5 min	
15% downhill grade at 48.3 km/h (30 mph) braking by generator action	
Air cooled from -30°C to +50°C ambient	
Battery voltage from 120 Vdc to 240 Vdc, with 180 Vdc preferred.	
Vehicle weight — 1361 kg (3000 lb)	
Frontal Area — 1.85 m ² (20 ft ²)	
Aerodynamic drag coefficient — 0.3	
Tire rolling resistance factor — 0.008	
Rolling radius — 0.292 m (0.96 ft)	
<i>Extracontractual</i>	
Mechanical Drive Train Efficiency	0.80 FM(A)
Correction for rotational inertia	0.95 FM(B)
Overspeed Factor	1.1 FM(A)
	1.2 FM(B)
	1.2

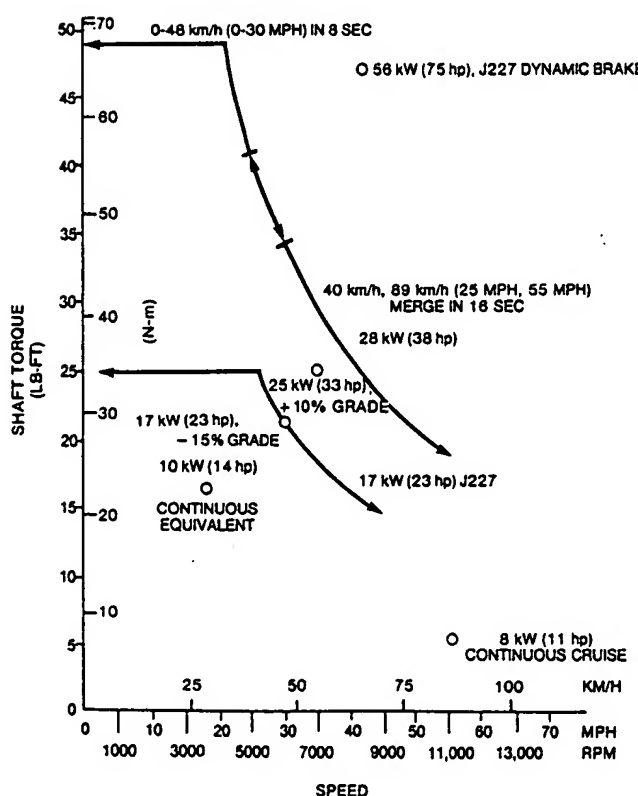


Figure 4. Revised Performance Requirements

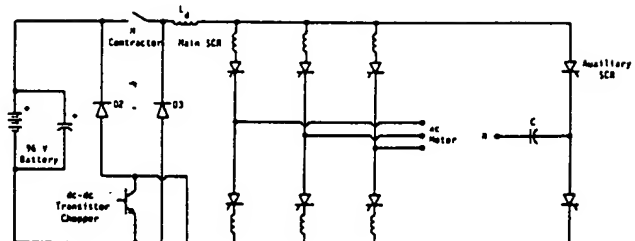


Figure 5. Load-Commutated Thyristor Inverter

tion of a single rotating disc machine. The magnets were to be contained in the rotor with a stator winding cast into the frames on each side of the rotor. A low-stress, limited performance, low-risk version of this motor was built and tested to demonstrate the principle of the method and to generate basic design data. This motor became known as the Proof-of-Principle (POP) motor.

The sketch in Figure 1 is a representation of the POP motor. The model shown in Figure 2 was built at full size from the POP motor drawings.

The stators of this motor were random wound and cast in a manner similar to that used for making the rotors of dc commutator disc motors. Each stator side case was machined from a solid piece of aluminum. The steel yoke and windings were cast in place with epoxy. The rotor hub was made from a single piece of aluminum by cutting shaped pockets to accept the large rare earth magnets. Typical magnet assemblies are shown, as set up for testing, in Figure 7. The magnets were epoxied into the hub and a 1-inch thick aluminum ring shrunk onto the

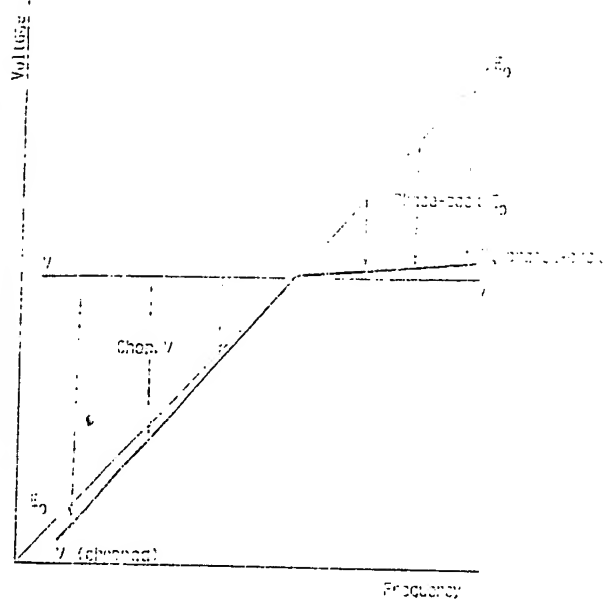


Figure 6. Illustration of Voltage Control Principle. Heavy lines show fixed V reduced by chopper and linear $E_o \approx E$, phased-back by inverter.

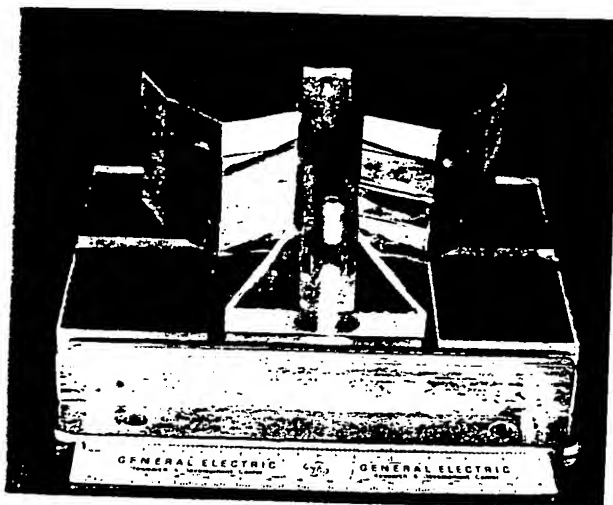


Figure 7. Magnet Test Fixture (POP)

assembly. This arrangement allowed operation up to 5000 rpm with safety. The principal dimensions of the POP motor are given in Table 2.

A comparison of measured and predicted equivalent circuit parameters is given in Table 3. The principal disagreement between prediction and test was in the open-circuit voltage. This was most likely due to actual differences in the magnets themselves because, for this motor, the poles were built up out of individually magnetized slabs which were not checked for quality. The magnetizing equipment pulse width and peak current were also not as large as desired.

A typical "V" curve measured with open loop sinewave drive on the POP motor is shown in Figure 8. The major difference in the predicted and measured curves is due to the discrepancy in open-circuit voltage.

Table 2
POP Motor Principal Dimensions

Rotor OD	28.5 cm (11.25 in.)
Magnet OD	23.5 cm (9.25 in.)
Magnet iD	13.0 cm (5.1 in.)
Rotor thickness	5.1 cm (2.0 in.)
Poles	8
Max. speed	5000 rpm
Overall length	11.7 cm (4.6 in.)
Overall diameter	31.8 cm (12.5 in.)
Total weight	41.5 kg (92.5 lb)

Table 3
POP Motor Parameters: 240 Hz
Estimated and Measured

	Estimate	Measured
Stator Resistance, r_1 (100°C) Ω	0.04	0.039
Direct-Axis Reactance, X_d Ω	0.08	0.081
Quadrature-Axis Reactance, X_q Ω	0.08	-
Subtransient Reactance, $X''_d = X''_q$, Ω	0.05	0.046
Open-Circuit Voltage, E_o (line), V	114	106.5

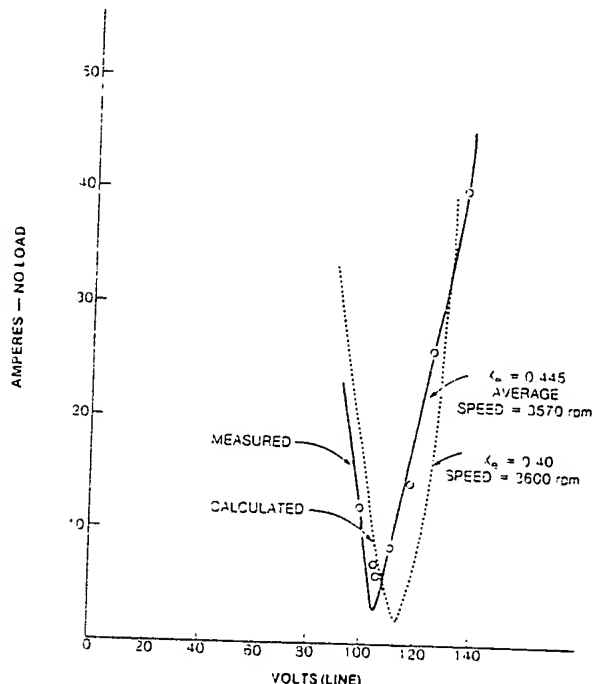


Figure 8. Variation of No-Load Amperes with Voltage-External Reactance in Line; Disk Motor, 5.2 kW (7 hp), 240 Hz, 8 Pole (POP Motor) - Sine Wave Drive

FUNCTIONAL MODEL MOTOR

After successful testing of the POP motor, a detailed analysis of the performance requirements was made. Then, utilizing the test experience of the POP motor, a full performance, fully stressed motor was designed, built, and tested. This was known as the Functional Model (FM) motor.

The original expectation for manganese-aluminum-carbon magnets was a low-cost material of 50% higher energy than ferrites. Since material cost was about \$0.60/lb, it was expected that the commercial price would be \$4-\$6/lb. In addition, the material was machinable to some extent, quite light, and had considerable mechanical strength. All of these factors appeared to make it a promising material for motors; hence the FM motor was designed with this material. Due to difficulties in the commercial availability of manganese aluminum carbon (MnALC) magnets, a special Alnico was fabricated to simulate its electromagnetic behavior. A comparison of CoSm rare earth, MnALC, and Alnico 8 is shown in Figure 9. The operating point of the magnets was close to the intersection of the Alnico 8 and MnALC curves.

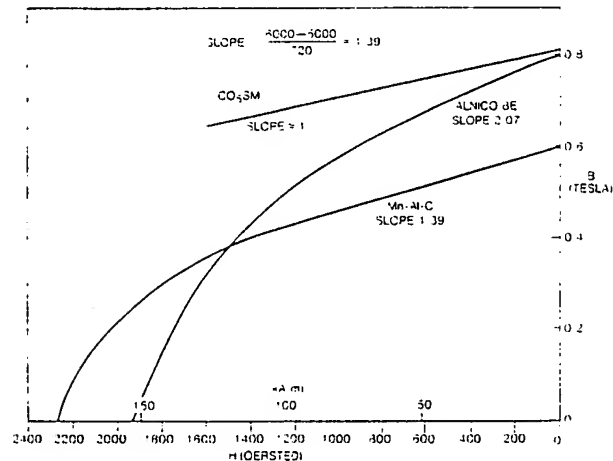


Figure 9. Comparison of CoSm, Alnico 8E with Mn-Al-C

A second change of plan occurred during the construction of the motor, when silicon steel was used for the yoke in place of amorphous iron. Amorphous iron was originally selected to give the least possible core losses and because no cutting of the tape was required for this motor, which ought to have made fabrication straightforward. In the first attempts to build the yokes, it became clear that this was a very difficult problem with amorphous iron. At the same time design studies were showing that the yoke losses were not an important factor in the total loss picture.

The winding was made in three separate but identical layers and placed on the yoke offset by 120° (electrical). The principal reason for this was to allow the automated fabrication of the coils outside of the motor. This also turned out to be more difficult than first thought, but the stators were eventually fabricated successfully.

Rotor construction was similar to that of the POP motor, except that the magnets were now full trapezoids with rounded bases and were supplied as fully built-up poles before magnetization. Magnetization was done after the motor was assembled by flashing two phases of the stator with a charged capacitor bank. The rotor containment was now a half-inch thick Inconel ring for safe running up to 11,000 rpm. The motor was equipped with cooling fins and fans so that steady-state operation under full load could be achieved.

A photograph of the finished motor is shown in Figure 10. The overall dimensions were, including cooling fins, 36.2 cm (14.25 in.) diameter and 19.7 cm (7.75 in.) length. Total weight was 53.1 kg (117 lb). A cross-section drawing of the motor is given in Figure 11.

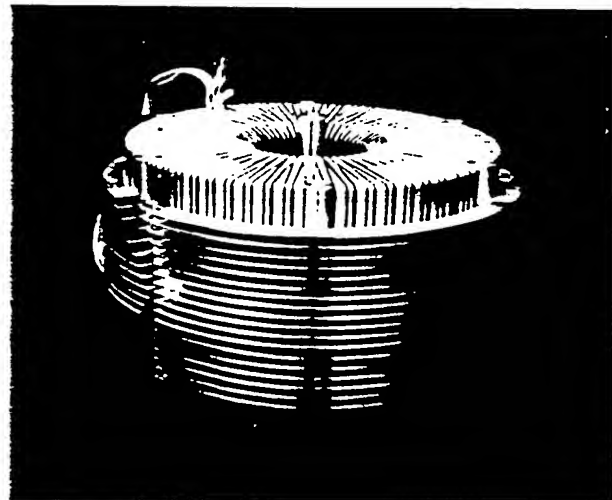


Figure 10. Completely Assembled Functional Model Motor

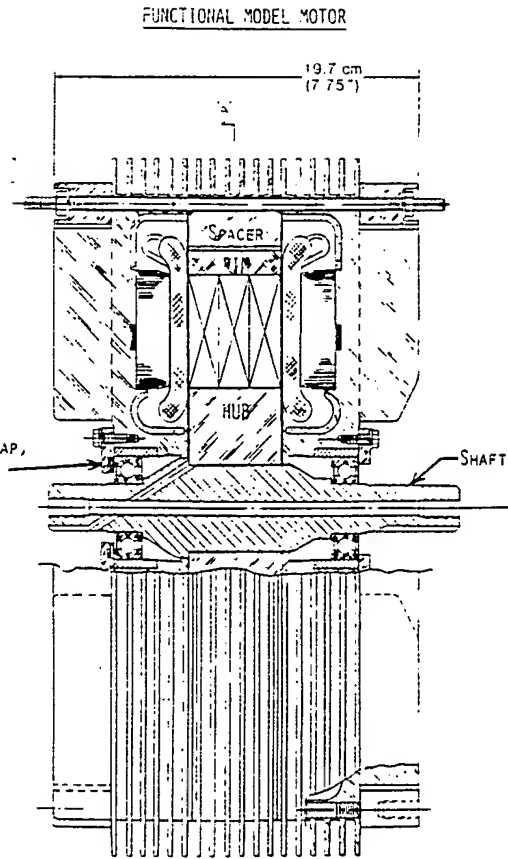


Figure 11. Cross Section of the Functional Model Motor

Both motors (FM and POP) were tested by generating into a resistance load (dynamic brake), open-loop motoring on sine wave at low power, and motoring at maximum power on a load-commutated inverter. This version of the FM motor did not perform as well as predicted in testing. The main problem was traced to the attempt at using permanent magnets with "soft" characteristics. That means the B-H curves in Figure 9 are sharply curving rather than a straight line as for the CoSm. This resulted in a loss of magnetization during high current loading and especially during inverter faults.

At the conclusion of testing, it was found that the magnets had lost one-third of their strength, which had a major effect on performance, especially in conjunction with the inverter load commutation. Secondary, but still important, problems were identified in winding balance as a result of the three-layer winding, wire size, and heat transfer. A thorough evaluation and redesign showed that all of these problems could be solved without increasing the size of the motor or changing the basic design concepts. The most important change was to switch to rare earth CoSm magnet material. This made economic, as well as technical sense, since Cobalt prices had dropped dramatically and the possibility of a low-cost cobalt-misch metal magnet now appeared realistic. A single-layer continuous chain winding with finer stranding and a precise locating system was substituted for the three-layer open windings. In addition to increased attention to finish and fit of the internal components, unique anisotropic metallic heat conductors were developed to rapidly remove heat from the end windings without incurring extra losses or compromising the insulation.

In an extension to the contract, all of these measures (and some others of a more minor nature) were implemented with outstanding success. The rotor (Figure 12) resembled the previous one but now utilized premagnetized blocks. Special care was taken to retain balance during construction to avoid balancing a magnetized rotor. Unbalance of less than 3.3 g-cm (0.046 oz-in.) was achieved by this method. The stator components of the FM(A) motor were reused for the FM(B) motor so that the appearance of the motor and the size are almost the same as shown in Figures 10 and 11. The internal details of the stator were, however, quite different. A view of one stator side before impregnation is shown in Figure 13. The principal dimensions of the FM(B) motor are given in Table 4.

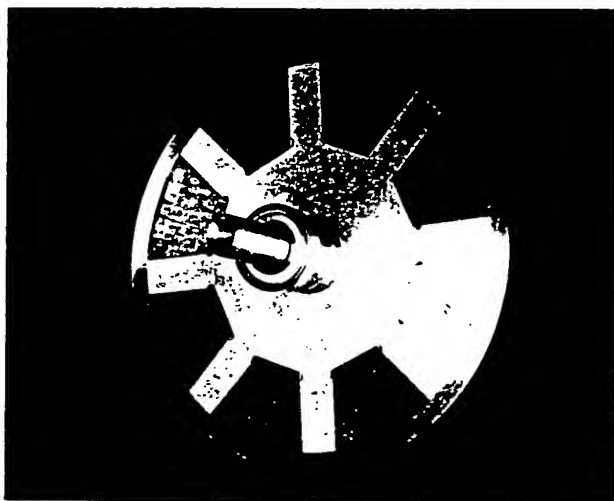


Figure 12. Finished Rotor - FM(B)

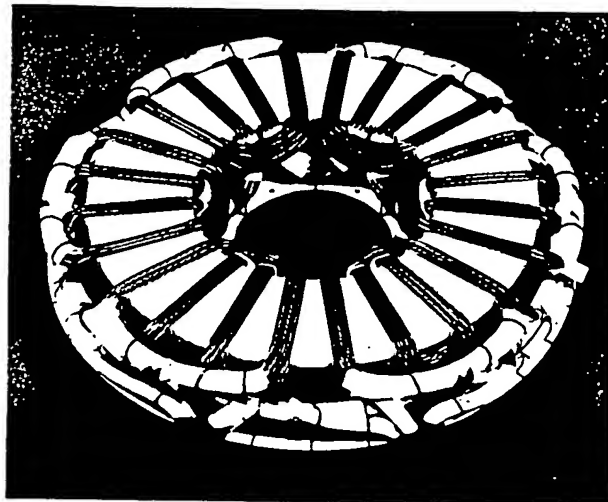


Figure 13. Stator Assembly Before Impregnation - FM(B)

Table 4

FM(B) Motor Principal Dimensions

Rotor OD	26.7 cm (10.52 in.)
Magnet OD	29.2 cm (9.54 in.)
Magnet ID	13.9 cm (5.47 in.)
Rotor thickness	3.9 cm (1.53 in.)
Poles	8
Max. speed	11,000 rpm
Overall length	20.8 cm (8.2 in.)
Overall diameter	36.2 cm (14.25 in.)
Total weight	58.2 kg (128 lb)

TEST RESULTS

Testing of the FM(B) motor consisted of parameter and balance checks, open circuit voltage, motoring on inverter drive, and generating into a resistance load. Open-circuit voltage balance was within $\pm 0.02\%$ on the three phases, inductance balance was within $\pm 0.5\%$, and resistance balance was within $\pm 0.3\%$. A comparison of the open-circuit voltage prediction and measurement is shown in Figure 14. A comparison of open-circuit predicted and measured losses is shown in Figure 15. The open circuit losses are the most difficult to predict and to control.

A great deal of detailed data was taken in all modes of operation and covering the entire range of motoring and braking within the capability of the power supplies. The performance of the motor exceeded the specification of the contract. A sample of this data is given on Tables 5 and 6.

Prediction with the refined model is quite close to experimental values over the entire range of loads and speeds. In generating to a resistance load, the voltage and current waveforms were almost sinusoidal (Figures 16 and 17), hence the prediction of the sinewave model was very close to measurement even for current. When operating as a motor on the load-commutated inverter, the current was close to an ideal 120° square wave and the voltage showed only very narrow and

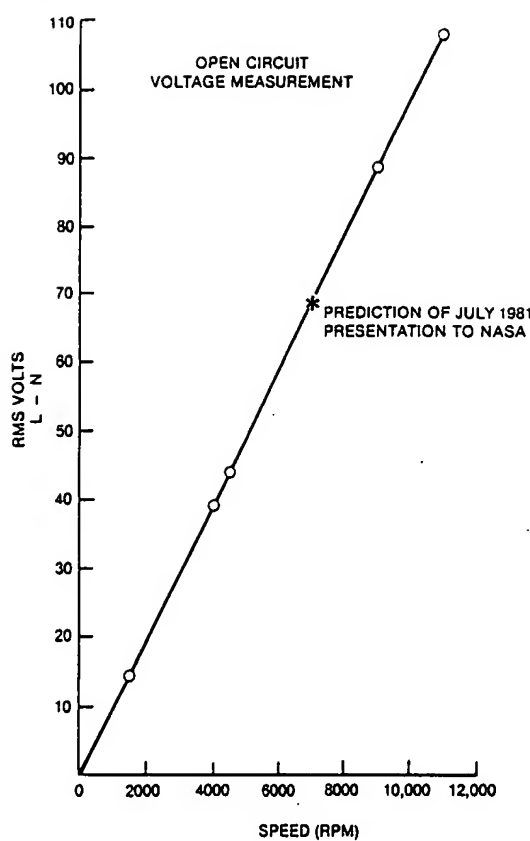


Figure 14. Open Circuit Voltage Measurement

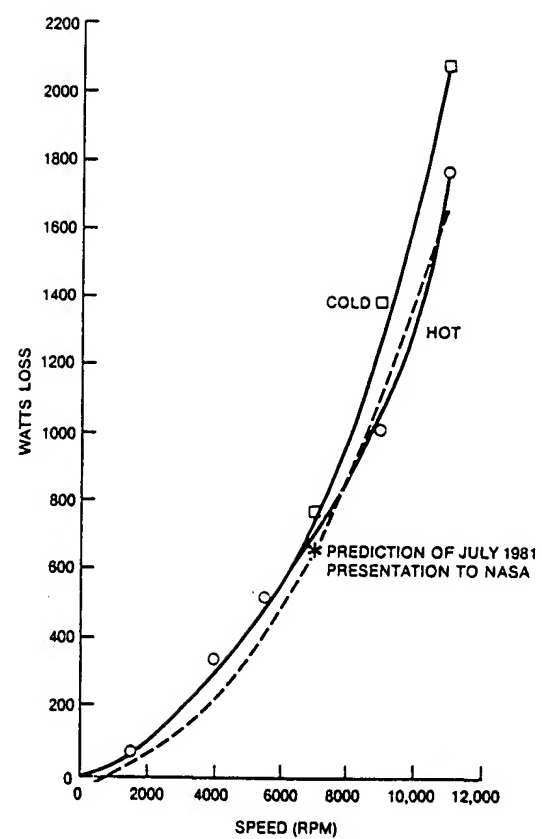


Figure 15. Open Circuit Loss Measurement

Table 5
Motoring Performance On Load-Commutated Inverter

Speed (rpm)	Shaft (hp)	Power Factor Angle (degrees)	Efficiency (%)	RMS Volts I-n ⁽¹⁾	RMS Amperes I ⁽²⁾	Winding Temperature Rise (°C) ⁽³⁾
4000	14.06	25.8(25.0)	91.1(91.1)	38.9(40.0)	99.4(107.9)	34.3(36.1)
6990	30.15	43.3(43.0)	87.7(87.9)	61.3(61.4)	173.4(192.8)	-
10,997	15.65	62.9(63.0)	81.3(81.8)	97.9(99.1)	97.3(104.7)	-

1. Calculated values based on sinewave model. Tested values are in parenthesis.
2. Sinewave prediction should be 0.935 times inverter case if waveform is ideal.
3. Data given for steady state heat runs only.

Table 6
Generating Performance With Resistance Load

Speed (rpm)	Shaft (hp)	Power Factor Angle (degrees)	Efficiency (%)	RMS Volts I-n	RMS Amperes I	Winding Temperature Rise (°C)
3998	14.41	-10.3(-10.0)	91.6(93.5)	36.6(36.9)	90.8(91.0)	26.8(25.5)
7091	43.70	-14.0(-14.0)	91.6(91.6)	63.6(63.5)	160.9(159.7)	-
11,005	15.33	-21.8(-22.0)	82.6(85.0)	105.8(105.3)	31.9(33.1)	-

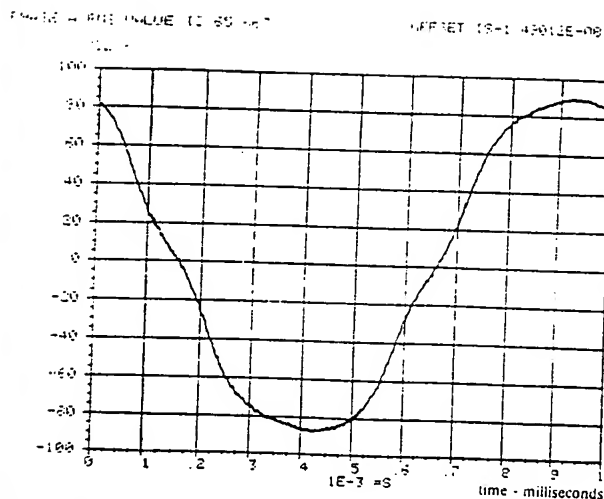


Figure 16. Phase A Voltage - Generating at 7000 rpm, 18.5 kW (24.8 hp)

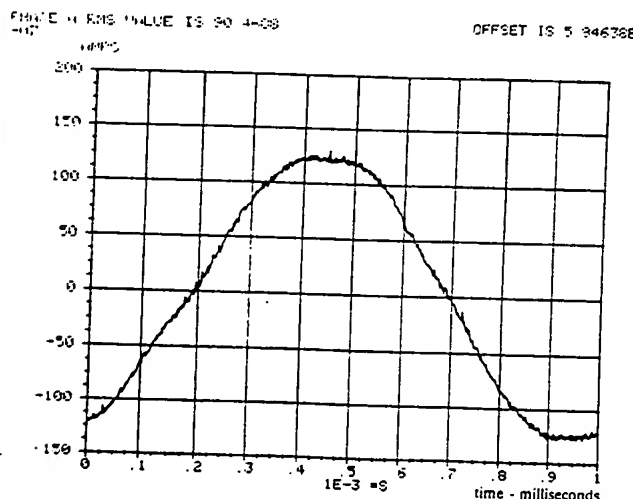


Figure 17. Phase A Current - Generating at 7000 rpm, 18.5 kW (24.8 hp)

small commutating notches even at the highest speeds (Figures 18 and 19) or at high power (Figures 20 and 21). If the current wave form were ideal, the measured rms current should be 1.07 times the fundamental or sinewave prediction, which is very nearly the case in Table 4.

At the conclusion of the required testing, an additional run was made to determine the peak efficiency. The result (Figure 22) shows an almost 93% maximum at 5000 rpm motoring on inverter drive while delivering 15hp (shaft). The refined model still slightly underestimates the efficiency. Proposed improvements would raise this peak to about 95% and shift it to about 20 hp.

At the conclusion of testing, an insulation failure occurred in the lead entry area in the motor casing. This has been attributed to a combination of inverter miscommutation and weakened insulation. Straightforward modification of the lead entry area and improved protection in the inverter should eliminate this problem.

The measurements were made using a large part of the system developed for the flywheel project and a digital processing oscilloscope. An overall view of the motor test stand and some of the instrumentation is shown in Figure 23. The motor,

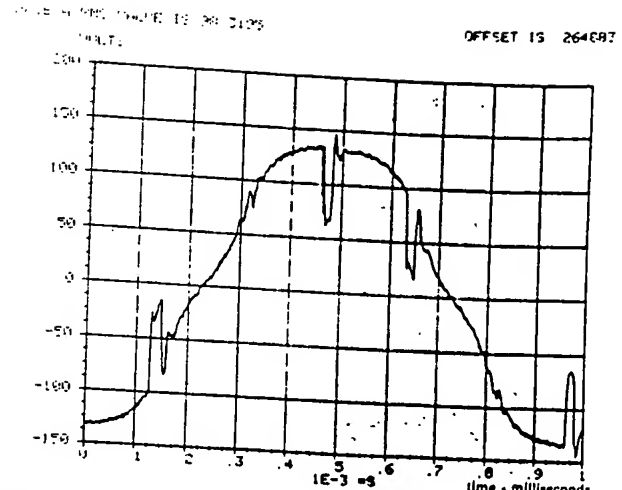


Figure 18. Phase A Voltage - Motoring at 11,000 rpm, 11.2 kW (15 hp)

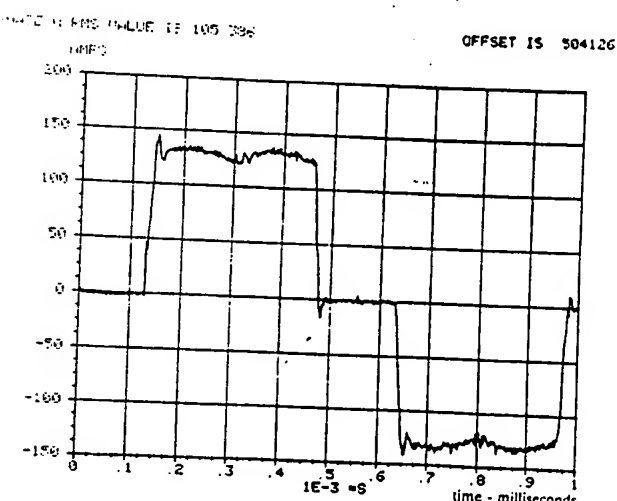


Figure 19. Phase A Current - Motoring at 11,000 rpm, 11.2 kW (15 hp)

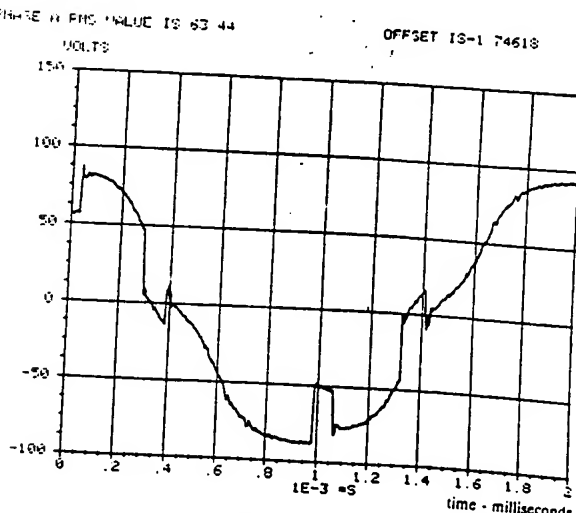


Figure 20. Phase A Voltage - Motoring at 7000 rpm, 23.9 kW (32 hp)

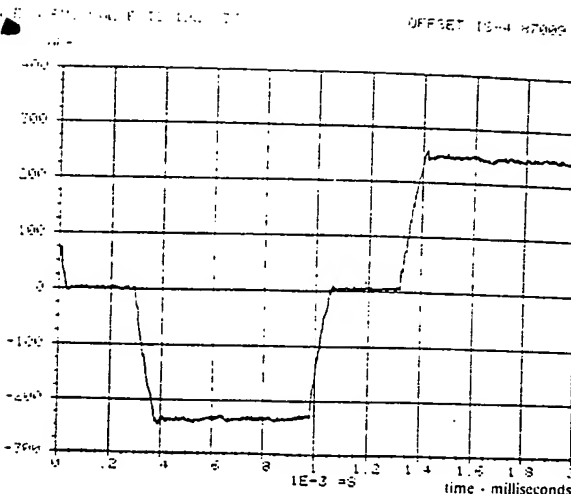


Figure 21. Phase A Current - Motoring at 7000 rpm, 23.9 kW (32 hp)

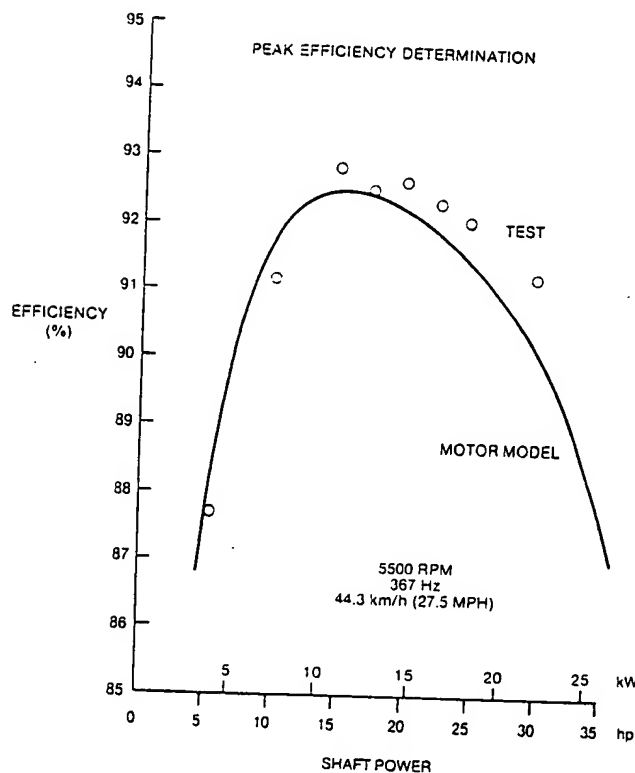


Figure 22. Peak Efficiency Determination

enclosed in its mounting/ventilation/safety frame, is at the center, the digital processing oscilloscope is at the right, and the vibration monitoring equipment is at the left.

CONCLUSIONS

A laboratory model of a high-speed permanent magnet axial flux disc motor for an electric passenger vehicle was successfully designed, built, and tested. The performance of the motor exceeded the requirements of the NASA/DOE contract under which it was built and showed promise of meeting the more demanding diesel-equivalent specification with some modification. Several relatively minor improvements were proposed to significantly raise the efficiency and reliability should

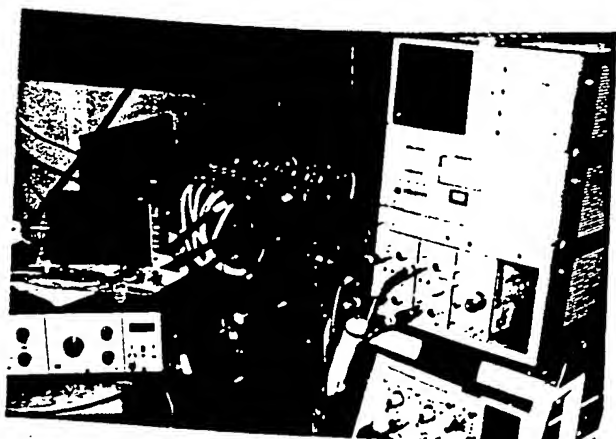


Figure 23. Test Setup Showing Terminals, Vibration Instrumentation, and Digital Processing Oscilloscope Cart

this type of development be continued. A detailed report on the entire project has been completed and will soon be available. (8)

ACKNOWLEDGMENTS

The author functioned as project manager and principal investigator for this development. Many others, including V.B. Honsinger, W.R. Oney, R.E. Tompkins, T.A. Nondahl, W.R. Mischler, A.B. Plunkett, M.J. Boyle, E. Whitley, M. VanDuyn, R.N. Johnson, O.H. Fraking, J. Cammarere, and the very capable machinists and technicians of the CRD shops, as well as B.R. Hatvani of NASA, contributed to this project.

REFERENCES

1. Plunkett, A.B. and Kliman, G.B., "Electric Vehicle AC Drive Development," SAE 800061, Congress and Exhibition, Detroit, MI, Feb. 1980.
2. General Electric Company, "Near Term Electric Vehicle Phase II Final Report," March 1980, DOE Contract No. DE-AC3-76CS51294.
3. Wilson, J.W.A., "The Drive System of the DOE Near Term Electric Test Vehicle (ETV-1)," Drive Electric '80, London, Oct. 1980.
4. Peak, S.C., "Improved Transistorized AC Motor Controller for Battery Powered Urban Electric Passenger Vehicles," Sept. 1982, Final Report General Electric Company, NASA CR-167978.
5. Peak, S.C. and Plunkett, A.B., "Transistorized PWM Inverter Induction Motor Drive System," IEEE-IAS Annual Meeting, San Francisco, Oct. 1982.
6. General Electric Company, "Regenerative Flywheel Energy Storage System," Vol. II Final Report, June 1980, Lawrence Livermore Laboratory subcontract #8990503.
7. Plunkett, A.B. and Turnbull, F.G., "Load Commutated Inverter/Synchronous Motor Drive Without a Shaft Positive Sensor," IEEE-IAS Trans., Vol IA-15, No. 1, Jan/Feb. 1979.
8. Kliman, G.B., "Advanced AC Permanent Magnet Axial Flux Disc Motor for Electric Passenger Vehicle," Oct. 1982 (in press). General Electric Company, NASA CR-167975.

This paper is subject to revision. Statements and opinions advanced in papers or discussion are the author's and are his responsibility, not SAE's; however, the paper has been edited by SAE for uniform styling and format. Discussion will be printed with the paper if it is published in SAE Transactions. For permission to publish this paper in full or in part, contact the SAE Publications Division.

Persons wishing to submit papers to be considered for presentation or publication through SAE should send the manuscript or a 300 word abstract of a proposed manuscript to: Secretary, Engineering Activity Board, SAE.

Printed in U.S.A.